

## ORIGINAL RESEARCH

# Starch degradation in the bean fruit pericarp is characterized by an increase in maltose metabolism

Lilia Bernal<sup>1</sup> | Eduardo Luján-Soto<sup>1</sup> | Carlos A. Fajardo-Hernández<sup>2</sup> |  
 Patricia Coello<sup>1</sup>  | Mario Figueroa<sup>2</sup> | Eleazar Martínez-Barajas<sup>1</sup> 

<sup>1</sup>Departamento de Bioquímica, Facultad de Química, Universidad Nacional Autónoma de México, Ciudad de México, Mexico

<sup>2</sup>Departamento de Farmacia, Facultad de Química, Universidad Nacional Autónoma de México, Ciudad de México, Mexico

**Correspondence**

Eleazar Martínez-Barajas, Departamento de Bioquímica, Facultad de Química, Universidad Nacional Autónoma de México Ciudad de México 04510, México.  
 Email: [emtz@unam.mx](mailto:emtz@unam.mx)

**Funding information**

Dirección General de Asuntos del Personal Académico, Universidad Nacional Autónoma de México, Grant/Award Numbers: IN222220, IN226520; Facultad de Química, UNAM, Grant/Award Numbers: PAIP 5000-9127, PAIP 5000-9145

Edited by H. Brumer

**Abstract**

The bean fruit pericarp accumulates a significant amount of starch, which starts to be degraded 20 days after anthesis (DAA) when seed growth becomes exponential. This period is also characterized by the progressive senescence of the fruit pericarp. However, the chloroplasts maintained their integrity, indicating that starch degradation is a compartmentalized process. The process coincided with a transient increase in maltose and sucrose levels, suggesting that  $\beta$ -amylase is responsible for starch degradation. Starch degradation in the bean fruit pericarp is also characterized by a large increase in starch phosphorylation, as well as in the activities of cytosolic disproportionating enzyme 2 (DPE2, EC 2.4.1.25) and glucan phosphorylase (PHO2, EC 2.4.1.1). This suggests that the rate of starch degradation in the bean fruit pericarp 20 DAA is dependent on the transformation of starch to a better substrate for  $\beta$ -amylase and the increase in the rate of cytosolic metabolism of maltose.

**1 | INTRODUCTION**

Starch is an important element in the metabolic strategies used by plants to cope with the negative effects of environmental variability. A large fraction of the carbon assimilated during the day is transiently stored as starch in chloroplasts and used to support metabolic needs during the night. Starch degradation has been extensively analyzed in *Arabidopsis* leaves. The available information shows that the process is under circadian control and subjected to additional regulation to meet the need for reduced carbon (C) levels during the night (Fernandez et al., 2017; Sulpice et al., 2014). Starch degradation in *Arabidopsis* leaves involves sequential phosphorylation of the C6 and C3 residues by glucan water dikinase (GWD) and phosphoglucan water dikinase (PWD), respectively (Hejazi et al., 2009; Ritte et al., 2006). Starch

phosphorylation alters the granule surface and facilitates its hydration (Hejazi et al., 2009). However, starch-bound phosphate can impede the movement of starch-degrading enzymes along the glucan chain and must be removed by the phosphoglucan phosphatases STARCH EXCESS4 (SEX4) and LIKE SEX FOUR2 (LSF2). SEX4 hydrolyses both C6- and C3-phosphate esters, whereas LSF2 is specific for glucans phosphorylated at C3 (Hejazi et al., 2010; Santelia et al., 2011).  $\beta$ -Amylases (EC 3.2.1.2.) catalyze the hydrolysis of  $\alpha$ -1,4-glycosidic bonds and release maltose from the exposed nonreducing end of the glucan chain. In the *Arabidopsis* genome, four genes encode chloroplast  $\beta$ -amylases (BAM1, -2, -3, and -4), with BAM1 and BAM3 being the most important for starch degradation (Fulton et al., 2008). ISOAMYLASE3 and LIMIT DEXTRINASE hydrolyze  $\alpha$ -1,6-glycosidic bonds and are required for removing branches. Maltose and glucose produced by starch

This is an open access article under the terms of the [Creative Commons Attribution-NonCommercial-NoDerivs](https://creativecommons.org/licenses/by-nc-nd/4.0/) License, which permits use and distribution in any medium, provided the original work is properly cited, the use is non-commercial and no modifications or adaptations are made.

© 2022 The Authors. *Physiologia Plantarum* published by John Wiley & Sons Ltd on behalf of Scandinavian Plant Physiology Society.

degradation are exported to the cytosol by the transporters MALT-  
 OSE EXCESS PROTEIN 1 (MEX1) and PLASTIDIC GLUCOSE  
 TRANSPORTER (pGlcT), respectively (Cho et al., 2011; Niittylä  
 et al., 2004). Cytosolic maltose is metabolized by disproportionat-  
 ing enzyme 2 (DPE2, Chia et al., 2004) and GLUCAN PHOSPHOR-  
 YLASE2 (PHO2, Fettke et al., 2004). DPE2 transfers one glucosyl  
 unit of maltose to a soluble glucan molecule and releases the other  
 for phosphorylation and sucrose synthesis (Chia et al., 2004;  
 Fettke et al., 2004). Cytosolic glucans are acted upon by glucan  
 phosphorylase (PHO2), releasing glucose 1-P (Fettke et al., 2004).  
 Nonphotosynthetic plastids also have the potential to synthesize  
 starch in response to sucrose availability (Hedhly et al., 2016).  
 Thus, starch acts as a “sugar source” when carbon is needed or as  
 a “sugar sink” when sugars are in excess (MacNeill et al., 2017).  
 This makes starch levels a good indicator of cellular carbon status  
 (Sulpice et al., 2009).

The pericarp of bean fruit has a prominent role in seed develop-  
 ment. This structure protects seeds and buffers against changes in  
 nutrient supply (Bennett et al., 2011); chloroplast differentiation into  
 amyloplasts in the mesocarp of the pod allows the use of surplus  
 sucrose in starch synthesis (Belmont et al., 2022). Starch degrada-  
 tion in the pericarp of bean fruit is not under circadian cycle control,  
 but starch is rapidly degraded when seed growth becomes exponen-  
 tial (Belmont et al., 2022). Since starch stored in the pericarp of  
 bean fruit appears to be important for later seed developmental  
 stages, it is necessary to understand the characteristics of this pro-  
 cess and how it is regulated. In this article, we describe the charac-  
 teristics of the starch degradation process in the pericarp of bean  
 fruit.

## 2 | MATERIALS AND METHODS

### 2.1 | Plant material

Seeds of the common bean (*Phaseolus vulgaris*) cv V8025 were sown  
 in Agrolyte and irrigated with a complete Hoagland nutrient solution  
 as described in Bernal et al. (2005). Plants were grown in a green-  
 house with natural light; the day temperatures ranged from 24 to  
 26°C, and the night temperatures ranged from 16 to 18°C. The  
 flowers were tagged at anthesis, and fruit age was defined in terms of  
 the number of days after anthesis (DAA). The analysis of the fruits  
 was performed after 20 DAA.

### 2.2 | Chlorophyll and carotene determination

Tissue (approximately 150 mg) was ground in liquid nitrogen, and 1 ml  
 of extraction solution (80% v/v acetone and 0.2 M Tris-HCl, pH 8)  
 was added. The material was mixed and centrifuged at 10,000 g for  
 10 min. The absorbance of the extract was measured at 647 and  
 664 nm and the chlorophyll and carotene concentrations were calcu-  
 lated according to Czarniecki et al. (2011).

### 2.3 | Carbohydrate analysis

Soluble sugars (glucose, fructose, and sucrose) and starch were  
 detected as previously reported (Bernal et al., 2005). The tissue was  
 homogenized in 80% (v/v) ethanol and incubated for 30 min at 80°C.  
 The extract was centrifuged at 12,000 g for 10 min, and the soluble  
 carbohydrates in the supernatant were detected using a Multiskan FC  
 microplate photometer (Thermo Fisher Scientific). The quantification  
 was performed in a sequential assay measuring NADH formation at  
 340 nm. In the first part of the reaction, 10–20 µl ethanol extract  
 was mixed with 150 µl reaction mixture (50 mM HEPES [pH 7.4],  
 50 mM KCl, 1 mM ATP, 3 mM MgCl<sub>2</sub>, 0.5 mM NAD<sup>+</sup>, and 1 U ml<sup>-1</sup>  
 yeast hexokinase [EC 2.7.1.1]). An initial reading was registered; then,  
 1.2 U ml<sup>-1</sup> glucose 6-P dehydrogenase (EC 1.1.1.49, from *Leuconos-  
 toc mesenteroides*) in 10 µl 50 mM HEPES (pH 7.4) was added. After  
 30 min, a second reading was obtained. The difference between the  
 first and second readings was used to calculate the glucose concentra-  
 tion. Then, 1.5 U ml<sup>-1</sup> phosphoglucose isomerase (EC 5.3.1.9, from  
 yeast) in 10 µl 50 mM HEPES (pH 7.4) was added, and another read-  
 ing was obtained after 30 min. The difference between the third and  
 second readings was used to calculate the fructose concentration.  
 Finally, 5 U ml<sup>-1</sup> invertase (EC 3.2.1.26) in 10 µl 50 mM HEPES  
 (pH 7.4) was added, and after 30 min, the final reading was registered.  
 The sucrose concentration was calculated based on the difference in  
 the readings after the addition of invertase and phosphoglucose isom-  
 erase. The ethanol-insoluble fraction was used for starch detection.  
 Pellets were suspended in 1 ml distilled water and incubated at 80°C  
 for 3 h. After cooling at room temperature, 250 U α-amylase  
 (EC 3.2.1.1) and 270 U amyloglucosidase (EC 3.2.1.3, from *Rhizopus*)  
 in 0.5 ml 0.25 M Na acetate buffer (pH 4.5) was added to each sam-  
 ple. After gentle mixing, the samples were incubated for 12 h at 37°C.  
 The next day, the samples were centrifuged at 12,000g for 10 min,  
 and glucose was measured in the supernatant by the enzymatic  
 method described above.

For maltose detection, ethanolic extracts were evaporated at  
 65°C and resuspended in water. Maltose was hydrolyzed in 90 mM  
 HEPES-NaOH (pH 7.5), 1 mM EDTA, and 2.5 U yeast maltase  
 (EC 3.2.1.20, Fluka 63412) in a 50 µl final reaction volume for 30 min  
 at 30°C. After heat inactivation, the glucose produced by maltase  
 treatment was enzymatically quantified.

### 2.4 | Purification of starch granules

Leaf starch granules were isolated according to Bernal et al. (2005).  
 Pods (15–20 g) were frozen with liquid nitrogen, ground in a cold  
 mortar, and homogenized in 50 ml extraction buffer (100 mM HEPES-  
 KOH (pH 8.0), 1 mM EDTA, 10 mM 2-mercaptoethanol, 1 mM PMSF,  
 1 mM benzamidine, and 2 mM aminocaproic acid). The homogenate  
 was filtered through four layers of cheesecloth and centrifuged for  
 5 min at 280 g. The pellet was washed twice in 10 ml extraction  
 buffer, resuspended in 1.5 ml extraction buffer, layered on top of a  
 5 ml Percoll cushion (95% Percoll; Pharmacia, and 5% (v/v) 0.5 M

HEPES-KOH (pH 7.0), and centrifuged for 5 min at 280g. The pellet was recovered and extensively washed with extraction buffer.

## 2.5 | LC-MS analysis of glucose 6-P from starch samples

Starch samples (duplicate) were hydrolyzed following the procedure described by Haebel et al. (2008). Briefly, each sample (10 mg) was treated with 1.0 ml 2 M trifluoroacetic acid (TFA) at 95°C for 3 h. Then, a 100  $\mu$ l aliquot of this solution was diluted with 500  $\mu$ l of water and dried under  $N_2$ . This process was repeated three times. Before derivatization, each sample was resuspended in 100  $\mu$ l water, and from these, a 30  $\mu$ l aliquot was brought to a volume of 401.5  $\mu$ l by adding 170  $\mu$ l water (MS grade), 200  $\mu$ l MeCN (MS grade), and 1.5  $\mu$ l 2 M HCl. The dry samples were kept at 4°C until derivatization. Derivatization of the glucose 6-P in the hydrolyzed starch samples was performed via a two-step reaction protocol (Rende et al., 2019). The dried samples were treated with 100  $\mu$ l methoxylamine, incubated on a heat block at 60°C for 30 min, and left overnight at room temperature. After this period, 30  $\mu$ l 1-methylimidazol and 60  $\mu$ l propionic acid anhydride were added. The reaction mixture was heated at 37°C for 30 min and then evaporated to dryness using  $N_2$ . A glucose 6-P standard (0.3 mg) was derivatized using the same procedure.

For LC-MS analysis, the derivatized products were resuspended in 100  $\mu$ l aqueous 0.1% formic acid (MS grade) and 7  $\mu$ l (19  $\mu$ g of derivatized samples) of each solution was injected. LC-MS analysis was performed on an Acquity UPLC system (Waters Inc.) coupled to an SQD2 mass spectrometer (Waters Inc.). For LC separation, a BEH  $C_{18}$  column (2.1  $\times$  100 mm, 1.7  $\mu$ m) at 40°C was employed. The mobile phase was composed of 0.1% methanol (A) and aqueous formic acid (B) using the following gradient: 0–60% A in 6 min; holding for 2 min; 60–100% A in 0.1 min; holding for 2 min; and returning to the starting conditions in 2 min. The flow rate was 0.3 ml  $min^{-1}$ , and MS data were collected through an electrospray ionization (ESI) source in negative mode over a full scan range ( $m/z$  50–2000). The instrument settings were as follows: capillary voltage, 4.0 kV; cone, 35 V; source temperature, 150°C; desolvation temperature, 350°C; cone gas flow, 10 L  $h^{-1}$ ; and desolvation gas flow, 500 L  $h^{-1}$ . Relative abundance ratios from the total ion chromatograms (TIC) at specific ion mass of  $m/z$  512 [glucose 6-P derivatized–H] $^-$  were extracted for all analyzed samples using MassLynx v4.1 software (Waters Inc.), and plotted using GraphPad Prism v.9.4.1 (GraphPad Software).

## 2.6 | PAGE and western blotting

Samples for electrophoresis were mixed with Laemmli denaturing buffer (Laemmli, 1970) and heated at 95°C for 5 min. SDS-PAGE and western blotting were performed according to Bernal et al. (2005). A rabbit antibody against  $\beta$ -amylase (NB 600-857, Novus Biologicals; diluted 1:10,000) and goat anti-rabbit antibody conjugated with HRP (diluted 1:20,000) were used. The blots were developed with

chemiluminescent HRP substrate (Millipore, Billerica, MA), and the antibody-antigen signal was detected using a ChemiDoc Image System from BioRad (Hercules).

## 2.7 | Enzymatic reactions

For determination of DPE2 and PHO2 activities, tissue was ground in liquid  $N_2$  and homogenized in 100 mM HEPES-Na OH (pH 7.5), 1 mM DTT, 1 mM EDTA, 15% glycerol, and complete protease inhibitor cocktail (Roche, Mannheim, DE). The extract was centrifuged at 10,000g for 5 min, and the supernatant was desalted in an NAP-10 column equilibrated with extraction buffer. Desalted extracts were used for enzymatic reactions.

The activity of DPE2 was measured as previously reported (Zeeman et al., 1998) with minor modifications. Briefly, the reaction mixture was composed of 100 mM HEPES-NaOH (pH 7.5), 2 mM maltose, and 2 mg  $ml^{-1}$  oyster glycogen. The assay was carried out for 30 min at 37°C and stopped by heat inactivation (5 min at 80°C). The glucose produced was enzymatically quantified in a reaction mixture containing 100 mM HEPES-NaOH (pH 7.5), 50 mM KCl, 3 mM  $MgCl_2$ , 1 mM ATP, 0.1 mM NAD, 1 U  $ml^{-1}$  yeast hexokinase, and 1 U  $ml^{-1}$  glucose 6-P dehydrogenase from *L. mesenteroides*. Controls were included to measure the glucose present in the desalted extract.

The activity of PHO2 was measured as indicated by Zeeman et al. (1998) with minor modifications. The reaction mixture contained 100 mM HEPES-NaOH (pH 7.5), 50 mM  $KH_2PO_4$ , and 2.5 mg  $ml^{-1}$  heat-denatured amylopectin. Assays were carried out for 30 min at 37°C and stopped by heat inactivation (5 min at 80°C). Glucose 1-P was enzymatically quantified in a reaction mixture composed of 100 mM HEPES-NaOH (pH 7.5), 50 mM KCl, 3 mM  $MgCl_2$ , 0.1 mM NAD, 1  $\mu$ M glucose 1,6-P, 1 U  $ml^{-1}$  phosphoglucose mutase (EC 5.4.2.2), and 1 U  $ml^{-1}$  glucose 6-P dehydrogenase from *L. mesenteroides*. Controls were included to measure the glucose 1-P present in the desalted extract.

The activities of  $\alpha$ - and  $\beta$ -amylase (EC 3.2.1.1 and EC 3.2.1.2, respectively) were determined in each fraction using the reagents Cer-alpha and Betamyl, respectively (Megazyme International).

## 2.8 | Purification of $\alpha$ -amylase

Fifty grams of bean pericarp at 30 DAA was ground with liquid  $N_2$  and homogenized with 250 ml extraction buffer (50 mM sodium acetate [pH 5.2], 1 mM  $MgCl_2$ , 1 mM  $CaCl_2$ , and 5 mM DTT). The extract was filtered through four layers of cheesecloth and centrifuged for 20 min at 12,000g. The supernatant was precipitated with ammonium sulfate at 30% saturation. After 1 h of incubation at 4°C, the precipitated proteins were recovered by centrifugation at 12,000 g for 20 min at 4°C. The proteins were resuspended in 20 ml extraction buffer, dialyzed against the extraction buffer for 24 h at 4°C and loaded onto a Q-Sepharose column (2  $\times$  10 cm) equilibrated in the same buffer. The bound proteins were eluted by a linear gradient of NaCl (0–0.5 M) at a flow rate of 1 ml  $min^{-1}$ ; 2 ml fractions were

collected, and  $\alpha$ -amylase activity was determined. The active fractions were precipitated with ammonium sulfate at 50% saturation for 5 h at 4°C. The precipitated proteins were recovered by centrifugation at 12,000 g for 20 min at 4°C; the pellet was resuspended in 5 ml extraction buffer, filtered through a 0.45 mm membrane filter (Corning Incorporated), and loaded onto a Sephacryl S-100 column (16/60) equilibrated with extraction buffer. Elution was performed at 1 ml min<sup>-1</sup>; 2 ml fractions were collected, and the activities of  $\alpha$ - and  $\beta$ -amylase were measured in the fractions.

## 2.9 | Protein mass spectrometry analysis

MS spectra were acquired on a Nano Acquity-LC\_ESI\_MS/MS mass spectrometer (quadrupole/time-of-flight, Synapt G2 High-Definition Mass Spectrometer, Waters Corporation). The data were analyzed using PLGS Explorer software (Waters Corporation) and the UniProt database. A peptide tolerance of 50 ppm, fragment mass tolerance of  $\pm 0.5$  Da, and peptide charge of +1 were selected. Only significant hits, defined as those with UniProt probability >95%, were accepted.

## 2.10 | Gel-based activity assays

Native gels were prepared as previously reported (Zeeman et al., 1998). To visualize total amylolytic activity, the gels contained 0.2% amylopectin and were run at 4°C and 50 V. When electrophoresis was completed, the gels were incubated overnight at room temperature and gently rocked in a solution containing 100 mM sodium acetate (pH 5.5). To reveal glucan phosphorylase activity, the gels including 0.8% oyster glycogen, were run at 4°C and 50 V and were incubated overnight in 100 mM Na-citrate (pH 6.5) and 20 mM glucose 1-P. In both cases, the gels were stained with Lugol (0.67% (w/v) I<sub>2</sub> and 3.33% (w/v) KI).

## 2.11 | Microscopy analysis

Bean pods were harvested at 20, 23, 25, 27, and 30 DAA. Then, 1-mm thick sections were dissected and fixed in a solution containing 3% (v/v) paraformaldehyde and 0.5% (v/v) glutaraldehyde in PBS (137 mM NaCl, 2.7 mM KCl, 10.9 mM Na<sub>2</sub>HPO<sub>4</sub> and 1.8 mM KH<sub>2</sub>PO<sub>4</sub>; pH 7.2) for 4 h at 4°C. The samples were then dehydrated and embedded in Epon:polypropylene oxide for 4 days. Thin sections were stained with safranin, and ultrathin sections (thickness 80 nm) were contrasted with 5% uranyl acetate and lead citrate solution. The sections were visualized with a Jeol 1200 EXII electron microscope (Jeol Ltd., <http://www.jeol.com>).

## 2.12 | RNA extraction

The samples were collected at 20, 23, 25, 27, and 30 DAA and immediately frozen in liquid nitrogen. Total RNA was isolated with TRIzol

(Thermo Fisher Scientific), and clean-up and concentration were performed using the RNA Clean and Concentrator TM-5 Kit (Zymo Research) according to the manufacturer's instructions. The RNA concentration was measured using Biodrop, and the quality of the total RNA was tested by agarose gel electrophoresis.

## 2.13 | Transcript quantification by RT-qPCR

Purified and DNase I-treated RNA was subjected to reverse transcription (RT) using oligo (dT) primers and the Ready Script Synthesis Mix (Sigma). Sequences were retrieved from Phytozome database (<https://phytozome-next.jgi.doe.gov>) and specific primers for each selected target were designed using Primer3Plus (Untergasser et al., 2007) with qPCR settings activated (Table S1). qPCR was performed using Maxima SYBR Green/ROX qPCR Master Mix in a CFX96 Touch real-time PCR system (Bio Rad). Relative expression levels were calculated using the 2<sup>- $\Delta\Delta$ Act</sup> method with the 20 DAA sample as a reference and actin transcript as an internal housekeeping control (Rao et al., 2013). Targets were assayed in at least three biological replicates with three technical replicates each ( $n \geq 9$ ).

## 2.14 | Statistical analysis

Data were analyzed using Prism software (GraphPad) and compared using a one-way analysis of variance (one-way ANOVA) with a Tukey multiple comparison post hoc test for determining significance.

# 3 | RESULTS

Bean fruit development (Figure 1A) is characterized by significant accumulation of starch, which was found to be reduced 20 DAA (Figure 1C). The fructose content was also reduced, while the glucose level remained almost constant (Figure 1D). At the same time, the amounts of sucrose and maltose showed a transient increase, and both were reduced at 25 DAA (Figure 1E). These results suggest that starch degradation involves the participation of  $\beta$ -amylase and that the product of starch degradation is used for sucrose synthesis.

Structural analysis of the bean fruit pericarp showed that at 20 DAA, the chloroplasts appeared to be filled with starch granules (Figure 2A). As the age of the fruit increased, the number and size of these organelles decreased (Figure 2). Simultaneously, the size and number of plastoglobules progressively increased (Figure 2). These structures are reliable markers of plastid senescence (Tamarly et al., 2019; Zechmann, 2019), and their presence and the reduction in the chlorophyll and carotene content (Figure 1B) are a clear indication of the senescence of the bean fruit pericarp during the seed developmental period. However, the structural analysis also showed that chloroplasts remained intact (Figure 2), suggesting that the starch degradation observed in the bean fruit pericarp was a compartmentalized process.

**FIGURE 1** Analysis of bean fruit pericarp during seed development. The amounts of chlorophyll and carotene (B), starch (C), glucose and fructose (D), and sucrose and maltose (E) were determined at the indicated stages of bean fruit development (A). The values correspond to the average of 10 determinations  $\pm$  SD. DAA, days after anthesis.

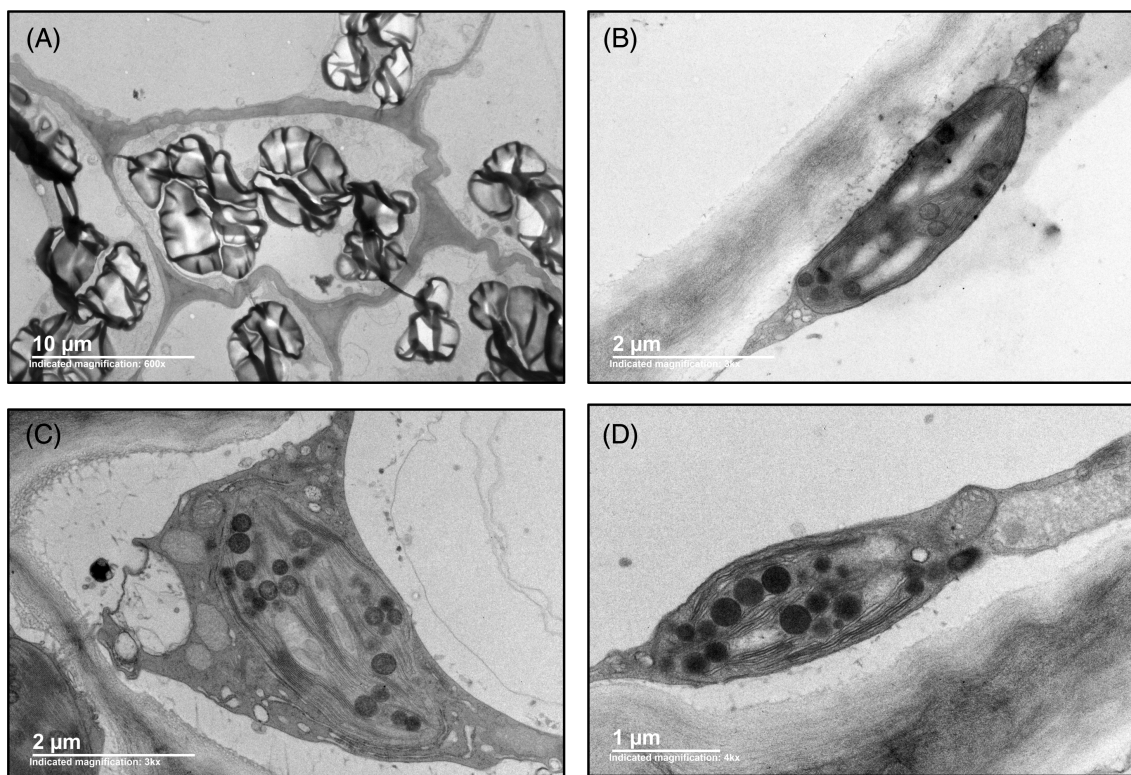
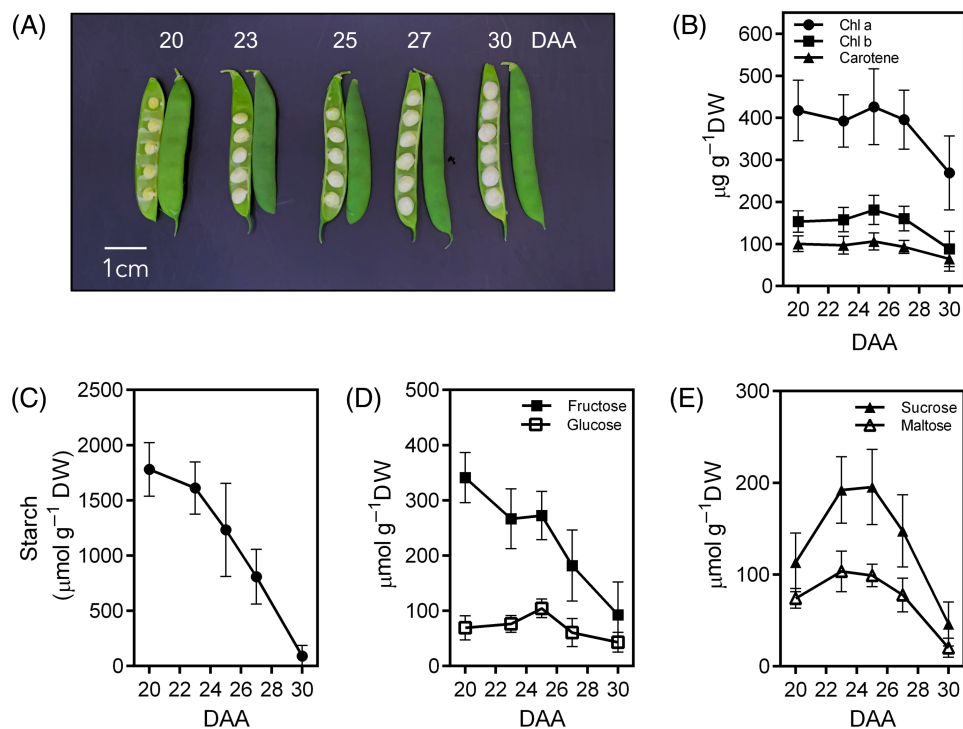


**FIGURE 2** Structural characteristics of chloroplasts. Representative images of chloroplasts in the bean fruit pericarp were obtained at 20 (A), 23 (B), 25 (C), and 30 (D) DAA. DAA, days after anthesis.

Therefore, to identify the characteristics of the amylases involved in this process, we evaluated the amylolytic activity of fruit pericarp extracts from 20 to 30 DAA in native gels using amylopectin as a

substrate. An increase in the intensity of the activity band located in the upper part of the gel was observed, while the intensity of the band detected in the middle part was gradually reduced (Figure 3A).

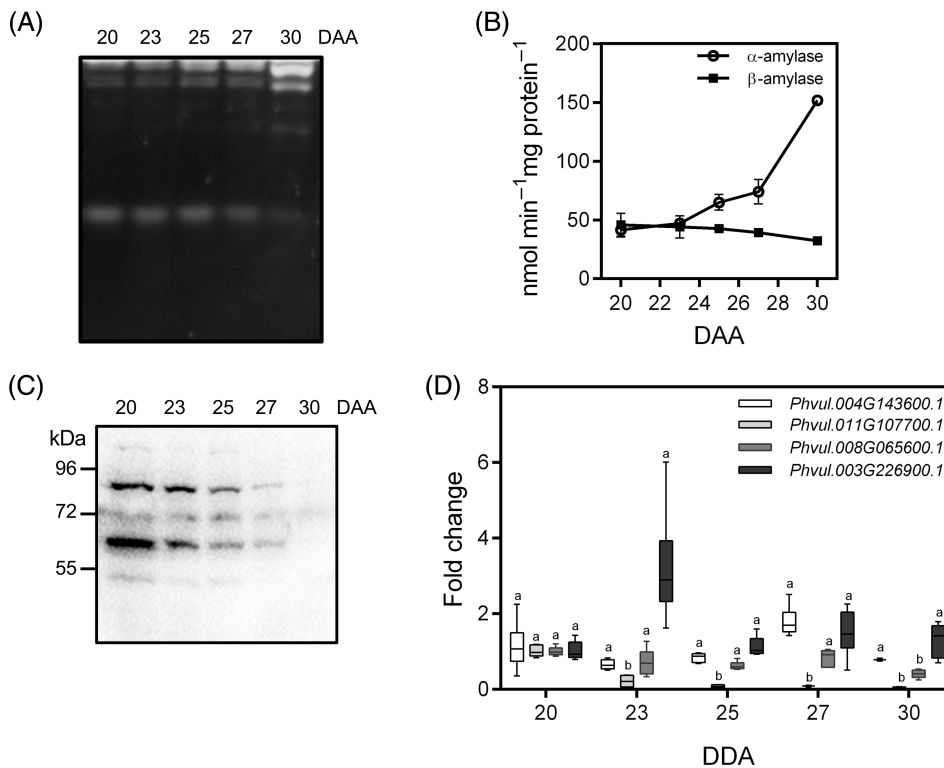


**FIGURE 3** Analysis of amylolytic activity in the bean fruit pericarp. Zymogram of amylolytic activity using oyster glycogen as a substrate (A), activities of  $\alpha$ - and  $\beta$ -amylase (B), western blot for  $\beta$ -amylase (C), and qPCR analysis of the expression of genes encoding  $\beta$ -amylases (D). The values of  $\alpha$ - and  $\beta$ -amylase activities (B) correspond to the average of five independent determinations  $\pm$  SD. The qPCR values (D) are the average of three biological samples, each evaluated in triplicate. DAA, days after anthesis. Letters indicate significant differences (Tukey test) at  $P \leq 0.01$

These changes correspond well with the increase in  $\alpha$ -amylase activity after 23 DAA and with the gradual reduction in  $\beta$ -amylase activity (Figure 3B). Western blot analysis using  $\beta$ -amylase-specific antibodies revealed the presence of two bands of 62 and 80 kDa whose intensity decreased as the fruit aged (Figure 3C). We also used qPCR to evaluate the expression of the genes *Phvul.003G226900*, *Phvul.004G143600*, *Phvul.008G065600*, and *Phvul.011G107700*, which encode  $\beta$ -amylases. After 23 DAA, we observed that the expression of *Phvul.003G226900* showed a transient increase, and the expression of *Phvul.004G143600* presented a small increase at 27 DAA. The expression of *Phvul.008G065600* was gradually reduced, and the expression of *Phvul.011G107700* was undetectable (Figure 3D). Information from the Phytozome database indicates that *Phvul.003G226900*, *Phvul.004G143600*, *Phvul.011G107700*, and *Phvul.008G065600* encode proteins of 61.5, 62.8, 55.9, and 78.2 kDa, respectively. This suggests that the 62 and 80 kDa bands detected by the  $\beta$ -amylase antibodies correspond to proteins encoded by the *Phvul.003G226900*, *Phvul.004G143600*, and *Phvul.008G065600* genes.

Under normal conditions,  $\alpha$ -amylase activity is not needed for leaf starch degradation (Yu et al., 2005); however, the chloroplast  $\alpha$ -amylase AMY3 plays an active role when the mechanism for starch degradation is perturbed (Streb et al., 2012), and its activity is important for starch degradation in guard cells (Flütsch et al., 2020). Due to the large differences between the bean fruit pericarp and leaves, we wanted to assess the role that the large increase in  $\alpha$ -amylase activity observed after 23 DAA (Figure 3B) might play in the degradation of the starch stored in this structure. To do so, we purified  $\alpha$ -amylase from pericarps at 30 DAA. Chromatography on Sephacryll S-100

allowed the separation of  $\alpha$ - and  $\beta$ -amylases (Figure 4A), and the fractions with high  $\alpha$ -amylase activity (fractions 44–50) were combined. Amylolytic activity analysis of this new fraction revealed a single band (Figure 4B), similar to the most intense band observed in the 30 DAA extracts (Figure 3A), and silver-stained SDS-PAGE revealed the presence of two bands of 45 and 32 kDa (Figure 4B). Both bands were analyzed by mass spectrometry, and the 45 kDa band was identified as an  $\alpha$ -amylase encoded by the gene *Phvul.010G017600* (Figure 4D).

We used qPCR to analyze the expression of *Phvul.001G001900*, *Phvul.003G069200*, *Phvul.008G033800*, and *Phvul.010G017600*, as these are genes of the *Phaseolus* genome that encode  $\alpha$ -amylases (Phytozome database). The expression of *Phvul.010G017600* consistently increased and peaked at 30 DAA; the expression of *Phvul.001G001900* also increased in the period from 27 to 30 DAA. At the same time, the expression of *Phvul.003G069200* and *Phvul.008G033800* did not show significant changes (Figure 4C). Taken together, these results indicate that the large increase in  $\alpha$ -amylase activity observed from 27 to 30 DAA (Figure 3B) could be attributed to the protein encoded by the gene *Phvul.010G017600*. According to the Phytozome database, this gene encodes an extracellular  $\alpha$ -amylase. The protein sequence was analyzed against the TMHMM server v 2.0 ([www.cbs.dtu.dk/services/TMHMM](http://www.cbs.dtu.dk/services/TMHMM), Hallgren et al., 2022), and the result was consistent with this hypothesis (Figure 4D). These findings, in addition to the fact that the increase in  $\alpha$ -amylase activity occurred when most of the starch had already been degraded (Figure 1), suggest that  $\alpha$ -amylase does not contribute to the degradation of the starch stored in the bean fruit pericarp. However, its activity could be important for the degradation of glucans liberated during tissue senescence.

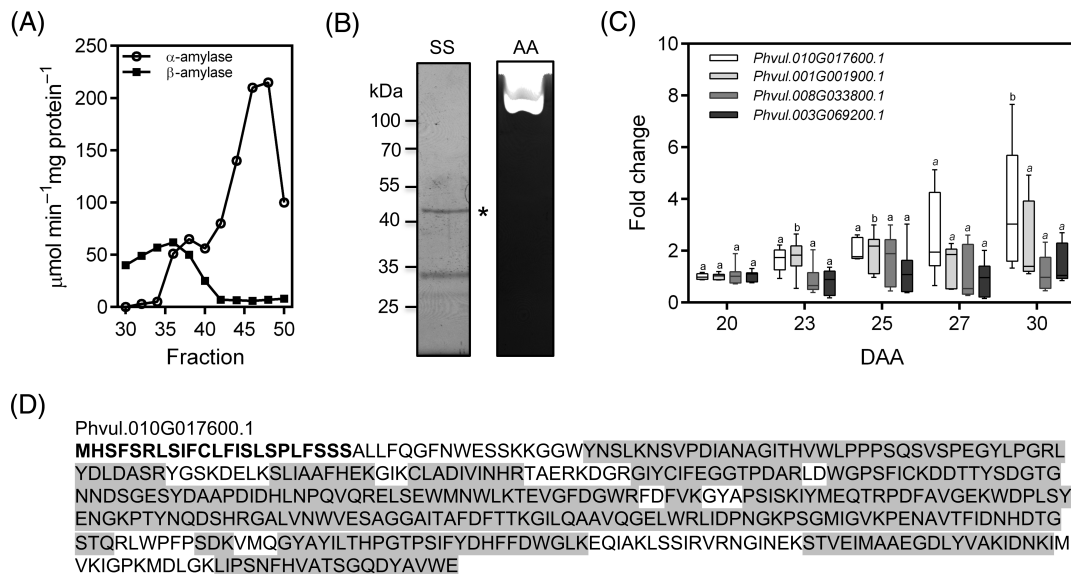
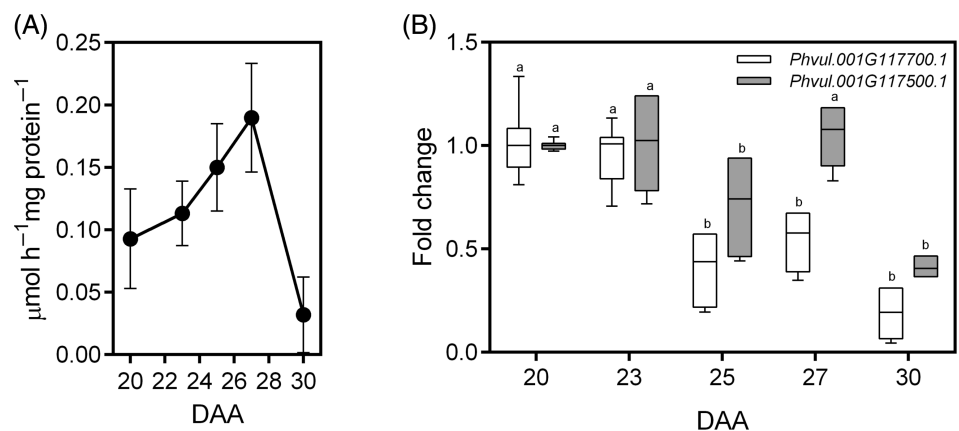


**FIGURE 4** Analysis of  $\alpha$ -amylase activity in the bean fruit pericarp. Separation of  $\alpha$ - and  $\beta$ -amylase by Sephacryll-S100 chromatography (a). The fractions with high  $\alpha$ -amylase activity (fractions 44–50 from Sephacryll-S100 chromatography) were pooled, separated by SDS-PAGE and silver stained (SS) or separated on native gels containing oyster glycogen to evaluate amylolytic activity (AA, B). qPCR analysis of the expression of genes encoding  $\alpha$ -amylases (C). Sequence of the 43 kDa protein deduced by mass spectrometry analysis (D). Bold letters in the protein sequence correspond to the predicted signal responsible for its secretion (TMHMM server, Hallgren et al., 2022). Shaded regions show peptides identified in the mass spectrometry analysis of the protein. The qPCR values (C) are the average of three biological samples, each evaluated in triplicate. \*, corresponds to the protein band identified as  $\alpha$ -amylase. Letters indicate significant differences (Tukey test) at  $P \leq 0.01$ . DAA, days after anthesis.

**FIGURE 5** Analysis of DPE2 activity. DPE2 activity in the bean fruit pericarp was evaluated using maltose and oyster glycogen as substrates (A), and qPCR analysis of genes encoding DPE2 (B). The activity values correspond to the average of five determinations  $\pm$  SD. The qPCR values are the average of three biological samples, each evaluated in triplicate. Letters indicate significant differences (Tukey test) at  $P \leq 0.01$ . DAA, days after anthesis.



DPE2 is important for the cytosolic metabolism of maltose produced by starch degradation. Figure 5A shows that its activity increased significantly from 20 to 27 DAA. In *P. vulgaris*, this protein is encoded by two genes, *Phvul.001G117700* and *Phvul.001G117500*. However, in contrast to the activity trend, the qPCR analysis indicated that the expression of both genes decreased. For *Phvul.001G117700*, the reduction started after 23 DAA, while the reduction in *Phvul.001G117500* expression became evident after 27 DAA (Figure 5B).

We also measured the activity of glucan phosphorylase to assess its contribution to starch degradation in the bean fruit pericarp. Figure 6A shows that glucan phosphorylase activity increased as starch was degraded (Figure 1C). The incubation of native gels

containing oyster glycogen with glucose 1-P was used to differentiate the activity of the chloroplast (PHO1) and cytosolic (PHO2) isoforms (Malinova et al., 2014). Figure 6B shows that after 20 DAA, the activity of the cytosolic isoform increased significantly, while the activity of the chloroplast isoform gradually decreased. Based on homology analysis with *Arabidopsis*, in *P. vulgaris*, PHO1 is encoded by *Phvul.004G034400* and PHO2 by *Phvul.006G064100*, and the expression of both transcripts was evaluated by qPCR. Figure 6C shows a transient increase in the expression of *Phvul.006G064100*, which peaked at 25 DAA and decreased thereafter. The expression of *Phvul.004G034400* also showed a modest increase. Altogether, these results indicate that the increase in glucan phosphorylase activity observed in the period where the starch stored in the pericarp was

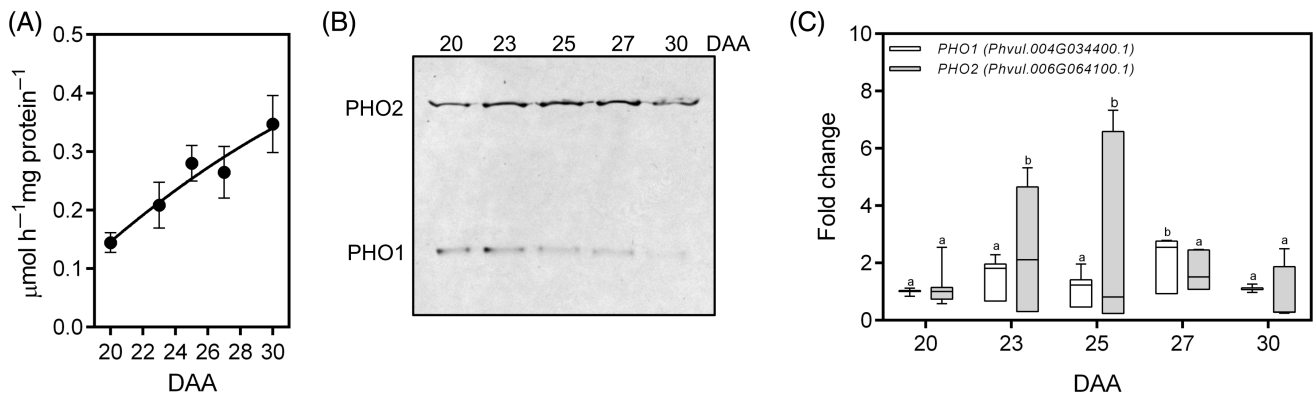


**FIGURE 6** Analysis of glucan phosphorylase. The activity of glucan phosphorylase present in the bean fruit pericarp was evaluated using heat denatured amylopectin as a substrate (A), or in native gels containing oyster glycogen and incubated with glucose 1-P (B). qPCR analysis of genes encoding chloroplast (PHO1) and cytosolic (PHO2) glucan phosphorylases (C). The activity values correspond to the average of five determinations  $\pm$  SD. The qPCR values are the average of three biological samples, each evaluated in triplicate. Letters indicate significant differences (Tukey test) at  $P \leq 0.01$ . DAA, days after anthesis.

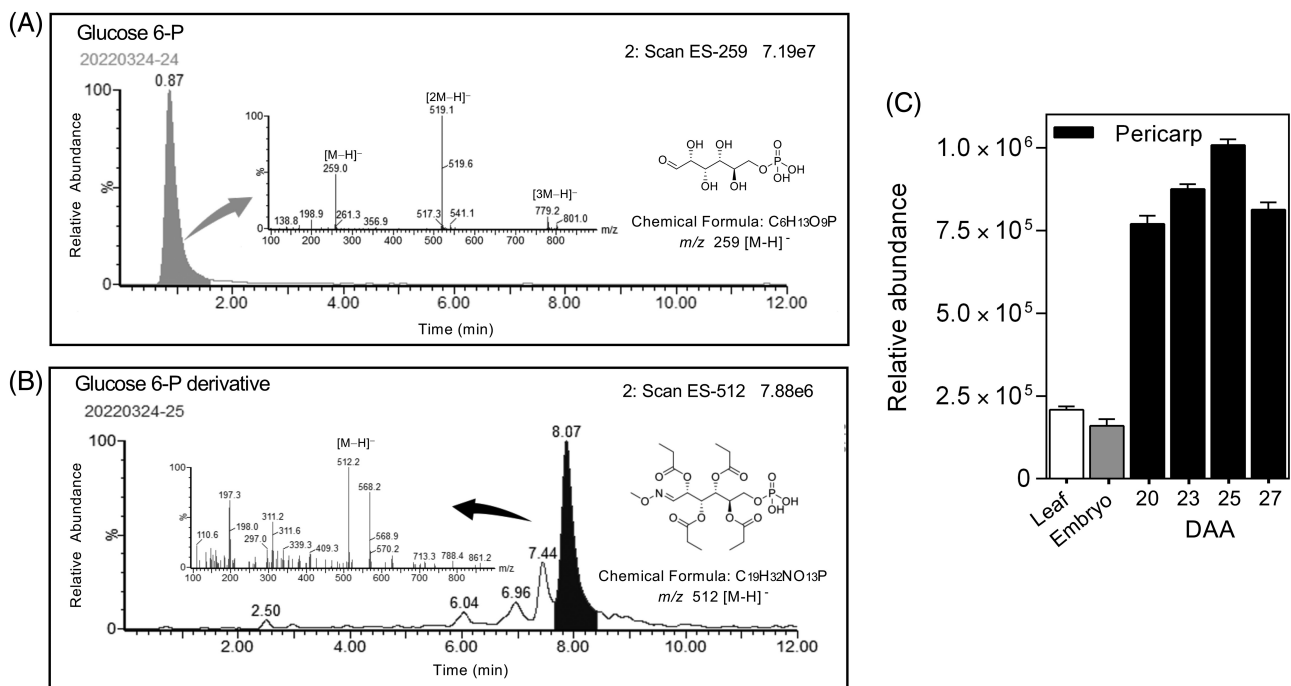


**FIGURE 7** LC-MS determination of glucose 6-P levels in starch samples. Extracted ion chromatograms of the glucose 6-P standard (A,  $m/z$  259  $[M-H]^-$ ) and the glucose 6-P derivatized product (B,  $m/z$  512  $[M-H]^-$ ). Relative abundance of glucose 6-P in derivatized starch samples isolated from leaves, embryos, and from bean fruit pericarp at 20, 23, 25, and 27 DAA was estimated by extracting the signal of  $m/z$  512  $[M-H]^-$  from the total ion chromatograms (C). Bars in panel C are the average of two biological samples  $\pm$  SD. DAA, days after anthesis.

degraded (Figure 6A) was the result of the increase in the expression of the gene *Phvul.006G064100*, which encodes the PHO2 isoform.

In *Arabidopsis* leaves, the transient phosphorylation at C6 and C3 of glucose molecules located on the surface of the starch granule is critical for starch degradation (Ritte et al., 2006). An LC-MS procedure based on the derivatization of glucose 6-P with methoxylamine (Figure 7A,B) was used to measure the relative amount of glucose 6-P present in starch isolated from the bean fruit pericarp. Our results indicated that the starch from the bean fruit pericarp was more

phosphorylated than starch samples isolated from leaf and embryo tissues (Figure 7C). On the other hand, the phosphorylation of starch from the bean fruit pericarp starch increased after 20 DAA, peaked at 25 DAA and then decreased (Figure 7C), suggesting that this modification did contribute to the starch degradation process. Starch phosphorylation is a transitory event, and the amount of phosphate present reflects the balance between the activities of the enzymes GWD and PWD responsible for the phosphorylation in the C6 and C3 positions of the glucose molecules, respectively (Hejazi et al., 2009;

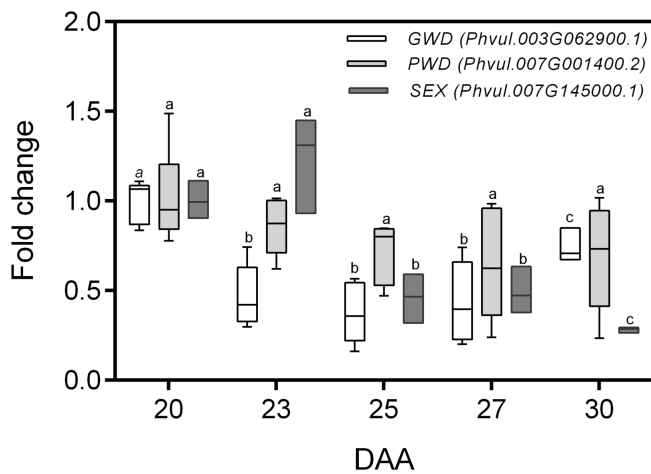


**FIGURE 8** qPCR analysis of the expression of genes encoding GWD, PWD, and SEX4. The qPCR values are the average of three biological samples, each evaluated in triplicate. Letters indicate significant differences (Tukey test) at  $P \leq 0.01$ . DAA, days after anthesis.

Ritte et al., 2006), and the phosphatases SEX and LSF2 that catalyze its dephosphorylation. SEX dephosphorylates C6 and C3, whereas LSF2 is specific for glucose phosphorylated at C3 (Hejazi et al., 2010; Santelia et al., 2011). qPCR analysis showed that the expression of genes encoding GWD (*Phvul.003G062900.1*) and PWD (*Phvul.007G001400.2*) decreased after 20 DAA, and the same was observed for SEX (*Phvul.007G145000.1*) expression after 23 DAA (Figure 8). These results suggest that the activity of these enzymes in the bean fruit pericarp determines the phosphorylation status of the starch granules, and this phenomenon is not regulated at the transcriptional level.

## 4 | DISCUSSION

Transient starch plays an important role in plant strategies to cope with carbon shortage. The clearest example is the degradation of the starch stored in leaves at night to support all kinds of metabolic needs. The plastids of almost all types of plant cells can synthesize starch in response to the availability of sucrose (Hedhly et al., 2016), and the use of starch is regulated by the needs of the plant (Sulspice et al., 2014; Weise et al., 2006). This makes starch a good indicator of the carbon status of the plant. We previously observed that chloroplasts in the bean fruit pericarp differentiate into amyloplasts (Figure 2A). This change allows the use of surplus sucrose for starch synthesis that is rapidly degraded when seed growth becomes exponential (Belmont et al., 2022), suggesting that starch degradation is promoted by a carbon deficit generated by the fast-growing seeds. Since starch degradation in the bean fruit pericarp is not under circadian control, it is very likely that some differences could exist in the process that has been described in leaves, as it has been reported that in *Arabidopsis*

guard cells, starch is rapidly degraded at dawn by  $\alpha$ -amylase 3 and  $\beta$ -amylase 1 in response to blue light signaling (Flütsch et al., 2020).

Our work shows that starch degradation in the bean fruit pericarp (Figure 1C) coincides with an increase in maltose and sucrose levels (Figure 1D), suggesting that  $\beta$ -amylase is responsible for starch degradation and the products used for sucrose synthesis. However, the process is characterized by a slight reduction in  $\beta$ -amylase activity and a large increase in  $\alpha$ -amylase activity (Figure 3B). The  $\alpha$ -amylase purified from the fruit pericarp at 30 DAA corresponded to the protein encoded by the gene *Phvul.010G017600*, whose expression increased after 23 DAA (Figure 4C). *Phvul.010G017600* is homologous to *Arabidopsis* AMY1 (*At4g25000*). AMY1 contains a signal sequence that allows transit through the rough endoplasmic reticulum and is then secreted from the cell in response to biotic and abiotic stress (Doyle et al., 2007). Analysis against the TMHMM server v 2.0 ([www.cbs.dtu.dk/services/TMHMM](http://www.cbs.dtu.dk/services/TMHMM), Hallgren et al., 2022) showed that *Phvul.010G017600* also contains a signal for extracellular secretion (Figure 4D). This, and the fact that the increase in  $\alpha$ -amylase activity occurred when most of the starch fruit pericarp had been degraded (Figures 1A and 3B), suggests that the increase in  $\alpha$ -amylase was associated with pericarp senescence and was not involved in the starch mobilization that started long before senescence symptoms became evident. Under normal conditions,  $\alpha$ -amylase is not involved in leaf starch degradation (Yu et al., 2005). Our results showed that the same occurs in the bean fruit pericarp. The bean fruit pericarp is a structure that undergoes progressive senescence during the seed developmental period. Plastoglobules are a reliable marker of the effect of this process on chloroplasts (Zechmann, 2019). The results presented in Figure 2 confirm this condition but also show that chloroplasts retain their integrity during all periods, suggesting that starch degradation in the fruit pericarp after 20 DAA is a compartmentalized process. In *Arabidopsis*, the degradation of leaf starch during the night relies on the activities of BAM1 and BAM3 (Fulton et al., 2008); the maltose produced is then exported to the cytosol by the transporter MEX1, where it is metabolized by DPE2 and glucan phosphorylase. DPE2 transfers one glucosyl unit of maltose to a cytosolic glucan and releases the other for phosphorylation and conversion to sucrose (Chia et al., 2004). Meanwhile, the action of PHO2 on cytosolic glucan produces glucose 1-P (Fettke et al., 2005). The fact that silencing of the genes encoding chloroplast-targeted  $\beta$ -amylases resulted in starch accumulation (Weise et al., 2006) and that DPE2 (Chia et al., 2004) and PHO2 (Qin et al., 2022) mutants had elevated starch, maltose, and hexose levels but low sucrose levels support this hypothesis.

Our work also shows that starch degradation (Figure 1C) coincides with an increase in the amount of glucose 6-P recovered from starch granules (Figure 7C). The changes induced by phosphorylation on the starch granule surface (Hejazi et al., 2009) could facilitate the activity of  $\beta$ -amylase (Fettke et al., 2009). The fact that the amount of glucose 6-P present in starch isolated from the bean fruit pericarp was approximately four times higher than the

amount present in starch isolated from leaves and embryos (Figure 7C) suggests that this modification can contribute significantly to increasing the efficiency of the process despite the reduction in  $\beta$ -amylase activity (Figure 3B,C). It has been reported that the reaction catalyzed by PHO2 is not needed for starch mobilization (Duwenig et al., 1997). However, *dpe2* mutants also show a significant increase in  $\beta$ -amylase and PHO2 activities (Chia et al., 2004), suggesting that an unexplored relationship between the two enzymatic activities might exist. We believe that the simultaneous increase in DPE2 (Figure 5A) and PHO2 (Figure 6B) activities increases maltose metabolism and facilitates the transfer of the product of starch degradation to developing seeds, as has been suggested to occur in *Arabidopsis* (Lu et al., 2006) or in some CAM plants, where maltose processing is critical for the use of starch (Ceusters et al., 2019).

An important question that needs to be answered is how seed development and starch degradation in fruit pericarp are coordinated. In *Arabidopsis* leaves, trehalose 6-P (Tre 6-P) is an inhibitor of the cytosolic part of the starch degradation process (Martins et al., 2013). Since Tre 6-P is also a specific indicator of sucrose status (Figueroa & Lunn, 2016), it has been proposed that the effect of Tre 6-P on starch degradation is important for balancing the rate of this process with the rate of sucrose export (Martins et al., 2013). We hypothesize that exponential seed growth reduces sucrose availability and Tre 6-P levels in the bean fruit pericarp, promoting the degradation of the starch stored in this structure. Finally, the fact that the degradation of the starch stored in leaf sheaths of rice plants contributes up to 30% to the grain yield (Okamura et al., 2018) indicates the relevance of the starch stored in the bean fruit pericarp in seed development. In conclusion, our work shows that the degradation of starch stored in the bean fruit pericarp occurs when seeds enter the rapid growth stage; the process is promoted by an increase in granule phosphorylation, which may facilitate the activity of  $\beta$ -amylase, and a simultaneous increase in the activities of DPE2 and PHO2, which accelerate the metabolic use of maltose.

## AUTHOR CONTRIBUTIONS

Lilia Bernal and Eduardo Luján-Soto performed qPCR analysis; Lilia Bernal, Patricia Coello, and Eleazar Martínez-Barajas did the biochemical analysis; Carlos A. Fajardo-Hernández and Mario Figueroa evaluated starch phosphorylation. Lilia Bernal, Patricia Coello, and Eleazar Martínez-Barajas analyzed the data and wrote the manuscript. Eleazar Martínez-Barajas designed the experiments. All authors have read and approved the final manuscript.

## ACKNOWLEDGMENTS

This work was supported by grants from UNAM-DGAPA-PAPIIT IN226520 (E M-B), FQ-PAIP 5000-9127 (E M-B), UNAM-DGAPA-PAPIIT IN222220 (MF) and FQ-PAIP 5000-9145 (MF). We thank Rodolfo Paredes Díaz for the microscopy analysis, and the anonymous reviewers that contributed to improving the quality of our work.

## DATA AVAILABILITY STATEMENT

The data that support the findings of this study are available from the corresponding author upon reasonable request.

## ORCID

Patricia Coello  <https://orcid.org/0000-0003-1858-8781>

Eleazar Martínez-Barajas  <https://orcid.org/0000-0002-0778-5248>

## REFERENCES

- Belmont, R., Bernal, L., Padilla-Chacón, D., Coello, P. & Martínez-Barajas, E. (2022) Starch accumulation in bean fruit pericarp is mediated by the differentiation of chloroplasts into amyloplasts. *Plant Science*, 316, 111163. Available from: <https://doi.org/10.1016/j.plantsci.2021.111163>
- Bennett, E.J., Roberts, J.A. & Wagstaff, C. (2011) The role of a pod in seed development: strategies for manipulating yield. *New Phytologist*, 190, 838–853.
- Bernal, L., Coello, P. & Martínez-Barajas, E. (2005) Possible role played by R1 protein in starch accumulation in bean (*Phaseolus vulgaris*) seedlings under phosphate deficiency. *Journal of Plant Physiology*, 162, 979–976.
- Ceusters, N., Frans, M., Van den Ende, W. & Ceusters, J. (2019) Maltose processing and not  $\beta$ -amylase activity curtails hydrolytic starch degradation in the CAM orchid *Phalaenopsis*. *Frontiers in Plant Science*, 10, 1386. Available from: <https://doi.org/10.3389/fpls.2019.01386>
- Chia, T., Thomeycroft, D., Chapple, A., Messerli, G., Chen, J., Zeeman, S.C. et al. (2004) A cytosolic glucosyltransferase is required for conversion of starch to sucrose in *Arabidopsis* leaves at night. *Plant Journal*, 37, 853–863.
- Cho, M.H., Lim, H., Shin, D.H., Jeon, J.S., Bhoo, S.H., Park, Y.I. et al. (2011) Role of the plastidic glucose translocator in the export of starch degradation products from the chloroplasts in *Arabidopsis thaliana*. *New Phytologist*, 190, 101–112.
- Czarnecki, O., Peter, E. & Grim, B. (2011) Methods for analysis of photosynthetic pigments and steady-state levels of intermediates of tetrapyrrole biosynthesis. In: Jarvis, R.P. (Ed.) *Chloroplasts research in Arabidopsis. Methods and protocols*, Vol. 2. Leicester, UK: Humana Press, pp. 357–385.
- Doyle, E.A., Lane, A.M., Sides, J.M., Mudgett, M.B. & Monroe, J.D. (2007) An  $\alpha$ -amylase (At4g25000) in *Arabidopsis* leaves is secreted and induced by biotic and abiotic stress. *Plant, Cell & Environment*, 30, 388–398.
- Duwenig, E., Steup, M., Willmitzer, L. & Kossmann, J. (1997) Antisense inhibition of cytosolic phosphorylase in potato plants (*Solanum tuberosum* L.) affects tuber sprouting and flower formation with only little impact on carbohydrate metabolism. *Plant Journal*, 12, 323–333.
- Fernandez, O., Ishihara, H., George, G.M., Mengin, V., Flis, A., Sumner, D. et al. (2017) Leaf starch turnover occurs in long days and in falling light at the end of the day. *Plant Physiology*, 174, 2199–2212.
- Fettke, J., Eckermann, N., Poeste, S., Pauly, M. & Steup, M. (2004) The glycan substrate of the cytosolic (Pho2) phosphorylase isozyme from *Pisum sativum* L.: identification, linkage analysis and subcellular localization. *Plant Journal*, 39, 933–946.
- Fettke, J., Hejazi, M., Smirnova, J., Höchel, E., Stage, M. & Steup, M. (2009) Eukaryotic starch degradation: integration of plastidial and cytosolic pathways. *Journal of Experimental Botany*, 60(10), 2907–2922.
- Fettke, J., Poeste, S., Eckermann, N., Tiessen, A., Pauly, M., Geigenberger, P. et al. (2005) Analysis of cytosolic heteroglycans from leaves of transgenic potato (*Solanum tuberosum* L.) plants under- or overexpress the Pho2 phosphorylase isozyme. *Plant Cell and Physiology*, 46(12), 1987–2004.
- Figueroa, C.M. & Lunn, J.E. (2016) A tale of two sugars: trehalose 6-phosphate and sucrose. *Plant Physiology*, 172, 7–27.

- Flütsch, S., Wang, Y., Takemiya, A., Vialet-Chabrand, R.M., Klejchová, M., Nigro, A. et al. (2020) Guard cell starch degradation yields glucose for rapid stomatal opening in *Arabidopsis*. *Plant Cell*, 32, 2325–2344.
- Fulton, D.C., Stettler, M., Mettler, T., Vaughan, C.K., Li, J., Francisco, P. et al. (2008)  $\beta$ -AMYLASE4, a noncatalytic protein required for starch breakdown, acts upstream of three active  $\beta$ -amylases in *Arabidopsis* chloroplast. *Plant Cell*, 20, 1040–1058.
- Haebel, S., Hejazi, M., Frohberg, C., Heydenreich, M. & Ritte, G. (2008) Mass spectrometric quantification of the relative amounts of C6 and C3 position phosphorylated glucosyl residues in starch. *Analytical Biochemistry*, 37, 73–79.
- Hallgren, J., Tsigirig, K.D., Pedersen, M.D., Almagro-Armenteros, J.J., Marcatili, P., Nielsen, H. et al. (2022) DeepTMHMM predicts alpha and beta transmembrane proteins using deep neural networks. *bioRxiv Preprint*. Available from: <https://doi.org/10.1101/2022.04.08.487609>
- Hedhly, A., Vogler, H., Schmid, M.W., Pazmino, D., Gagliardini, V., Santelia, D. et al. (2016) Starch turnover and metabolism during flower and early embryo development. *Plant Physiology*, 172, 2388–2402.
- Hejazi, M., Fettke, J., Kötting, O., Zeeman, S.C. & Steup, M. (2010) The laforin-like dual-specificity phosphatase SEX4 from *Arabidopsis* hydrolyzes both C6- and C3-phosphate esters introduced by starch-related dikinases and thereby affects phase transition of alpha-glucans. *Plant Physiology*, 152, 711–722.
- Hejazi, M., Fettke, J., Paris, O. & Steup, M. (2009) The two plastidial starch-related dikinases sequentially phosphorylate glucosyl residues at the surface of both the A- and B-type allomorphs of crystallized maltodextrins but the mode of action differs. *Plant Physiology*, 150, 962–976.
- Laemmli, U.K. (1970) Cleavage of structural proteins during the assembly of the head of bacteriophage T4. *Nature*, 227, 680–685.
- Lu, Y., Steichen, J.M., Weise, S.E. & Sharkey, T.D. (2006) Cellular and organ level localization of maltose in maltose-excess *Arabidopsis* mutants. *Planta*, 224, 935–943.
- MacNeill, G.J., Mehrpouyan, S., Minow, M.A., Patterson, J.A., Tetlow, I.J. & Emes, M.J. (2017) Starch as a source, starch as a sink: the bifunctional role of starch in carbon allocation. *Journal of Experimental Botany*, 68(16), 4433–4453.
- Malinova, I., Mahlow, S., Alseekh, S., Orawetz, T., Fernie, A.R., Baumann, O. et al. (2014) Double knockout mutants of *Arabidopsis* grown under normal conditions reveal that the plastidial phosphorylase isozyme participates in transitory starch metabolism. *Plant Physiology*, 164, 907–921.
- Martins, M.C.M., Hejazi, M., Fettke, J., Steup, M., Feil, R., Krause, U. et al. (2013) Feedback inhibition of starch degradation in *Arabidopsis* leaves mediated by trehalose-6-phosphate. *Plant Physiology*, 163, 1142–1163.
- Niittylä, T., Messlerli, G., Trevisan, M., Chen, J., Smith, A.M. & Zeeman, S.C. (2004) A previously unknown maltose transporter essential for starch degradation in leaves. *Science*, 303, 87–89.
- Okamura, M., Arai-Sanoh, Y., Yoshida, H., Mukouyama, T., Adachi, S., Yabe, S. et al. (2018) Characterization of high-yielding rice cultivars with different grain-filling properties to clarify the limiting factors for improving yield. *Field Crops Research*, 219, 139–147.
- Qin, Y., Xiao, Z., Zhao, H., Wang, J., Wang, Y. & Qiu, F. (2022) Starch phosphorylase 2 is essential for cellular carbohydrate partitioning in maize. *Journal of Integrative Plant Biology*, 64, 1755–1769. Available from: <https://doi.org/10.1111/jipb.13328>
- Rao, X., Huang, X., Zhou, Z. & Lin, X. (2013) An improvement of the 2<sup>-</sup> $\Delta\Delta$ CT method for quantitative real-time polymerase chain reaction data analysis. *Biostatistics, Bioinformatics and Biomathematics*, 3, 71–85.
- Rende, U., Niittylä, T. & Moritz, T. (2019) Two-step derivatization for determination of sugar phosphates in plants by combined reversed phase chromatography/tandem mass spectrometry. *Plant Methods*, 15, 127. Available from: <https://doi.org/10.1186/s13007-019-0514-9>
- Ritte, G., Heydenreich, M., Mahlow, S., Haebel, S., Kötting, O. & Steup, M. (2006) Phosphorylation of C6 and C3-positions of glucosyl residues in starch is catalyzed by distinct dikinases. *FEBS Letters*, 580, 4872–4876.
- Santelia, D., Kötting, O., Seung, D., Schubert, M., Thalman, M., Bischof, S. et al. (2011) The phosphoglucan phosphatase like sex four2 dephosphorylates starch at the C3-position in *Arabidopsis*. *Plant Cell*, 23, 4096–4111.
- Streb, S., Eicke, S. & Zeeman, S.C. (2012) The simultaneous abolition of three starch hydrolases blocks transient starch breakdown in *Arabidopsis*. *Journal of Biological Chemistry*, 287, 41745–41756.
- Sulpice, R., Pyl, E.T., Ishihara, H., Trenkamp, S., Steinfath, M., Witucka-Wall, H., Gibon, Y. et al. (2009) Starch as a major integrator in the regulation of plant growth. *Proceedings of the National Academy of Sciences of the United States of America*, 106(25), 10348–10353.
- Sulpice, R., Flis, A., Ivakov, A.A., Apelt, F., Krohn, N., Encke, B. et al. (2014) *Arabidopsis* coordinates the diurnal regulation of carbon allocation and growth across a wide range of photoperiods. *Molecular Plant*, 7, 137–155.
- Tamary, E., Nevo, R., Naveh, L., Levin-Zaidman, S., Kiss, V., Savidor, A. et al. (2019) Chlorophyll catabolism precedes changes in chloroplast structure and proteome during leaf senescence. *Plant Direct*, 3, e00127. Available from: <https://doi.org/10.1002/pld3.127>
- Untergasser, A., Nijveen, H., Rao, X., Bisseling, T., Geurts, R. & Leunissen, J.A. (2007) Primer3Plus, an enhanced web interface to Primer3. *Nucleic Acids Research*, 35, W71–W74. Available from: <https://doi.org/10.1093/nar/gkm306>
- Weise, S.E., Schrader, S.M., Kleinbeck, K.R. & Sharkey, T.D. (2006) Carbon balance and circadian regulation of hydrolytic and phospholytic breakdown of transitory starch. *Plant Physiology*, 141, 879–886.
- Yu, T.-S., Zeeman, S.C., Thorneycroft, D., Fulton, D.C., Dunstan, H., Lue, W.-L. et al. (2005)  $\alpha$ -Amylase is not required for breakdown of transitory starch in *Arabidopsis* leaves. *Journal of Biological Chemistry*, 280(11), 9773–9779.
- Zechmann, B. (2019) Ultrastructure of plastids serves as a reliable abiotic and biotic stress marker. *PLoS One*, 14(4), e0214811. Available from: <https://doi.org/10.1371/journal.pone.0214811>
- Zeeman, S.C., Northrop, F., Smith, A.M. & Rees, T. (1998) A starch-accumulating mutant of *Arabidopsis thaliana* deficient in chloroplastic starch-hydrolysing enzyme. *Plant Journal*, 15, 357–365.

## SUPPORTING INFORMATION

Additional supporting information can be found online in the Supporting Information section at the end of this article.

**How to cite this article:** Bernal, L., Luján-Soto, E., Fajardo-Hernández, C.A., Coello, P., Figueroa, M. & Martínez-Barajas, E. (2022) Starch degradation in the bean fruit pericarp is characterized by an increase in maltose metabolism. *Physiologia Plantarum*, 174(6), e13836. Available from: <https://doi.org/10.1111/ppl.13836>